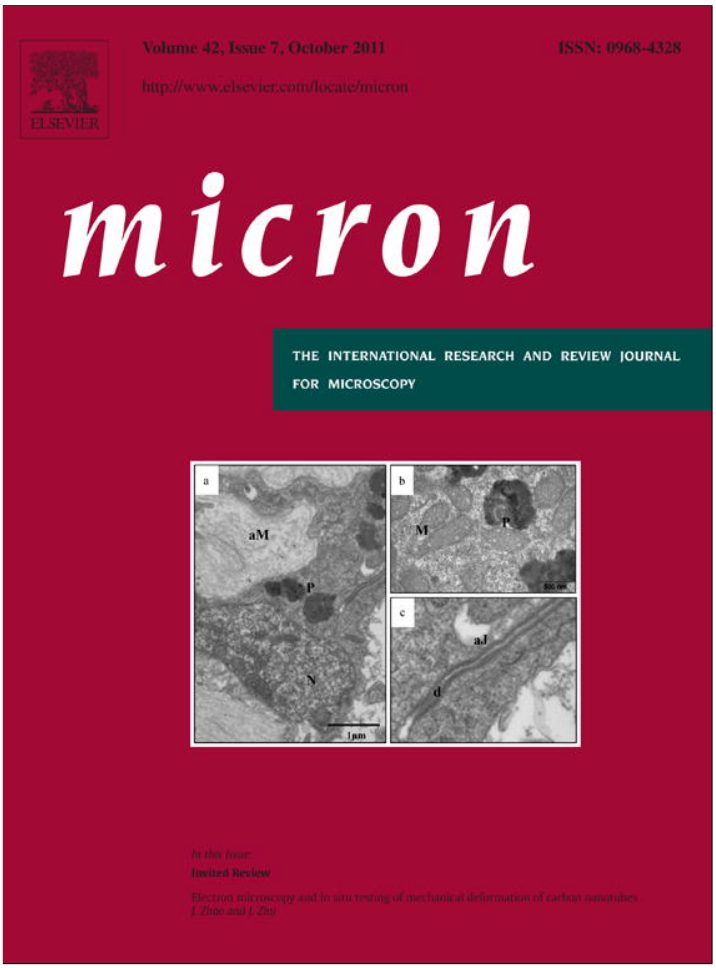

Micron 42 (2011) 680–690

Contents lists available at ScienceDirect

Micron

journal homepage: www.elsevier.com/locate/micron

Ultrastructural description of spermiogenesis within the Mediterranean Gecko, *Hemidactylus turcicus* (Squamata: Gekkonidae)

Justin L. Rheubert[a,*], Dustin S. Siegel[b], Katherine J. Venable[c], David M. Sever[a], Kevin M. Gribbins[c]

[a] Department of Biological Sciences, Southeastern Louisiana University, SLU 10736, Hammond, LA 70402, USA
[b] Department of Biology, Saint Louis University, St. Louis, MO 63103, USA
[c] Department of Biology, Wittenberg University, PO Box 720, Springfield, OH 45501, USA

ARTICLE INFO

Article history:
Received 6 January 2011
Received in revised form 10 March 2011
Accepted 11 March 2011

Keywords:
Sperm
Development
Gecko
Gamete

ABSTRACT

We studied spermiogenesis in the Mediterranean Gecko, *Hemidactylus turcicus*, at the electron microscope level and compared to what is known within other Lepidosaurs. In *H. turcicus* germ cells are connected via cytoplasmic bridges where organelle and cytoplasm sharing is observed. The acrosome develops from merging transport vesicles that arise from the Golgi and subsequently partition into an acrosomal cap containing an acrosomal cortex, acrosomal medulla, perforatorium, and subacrosomal cone. Condensation of DNA occurs in a spiral fashion and elongation is aided by microtubules of the manchette. A nuclear rostrum extends into the subacrosomal cone and is capped by an epinuclear lucent zone. Mitochondria and rough endoplasmic reticulum migrate to the posterior portion of the developing germ cell during the cytoplasmic shift and the flagellum elongates. Mitochondria surround the midpiece as the anlage of the annulus forms. The fibrous sheath begins at mitochondrial tier 3 and continues into the principal piece. Peripheral fibers associated with microtubule doublets 3 and 8 are grossly enlarged. During the final stages of germ cell development spermatids are wrapped with a series of Sertoli cell processes, which exhibit ectoplasmic specializations and differing cytoplasmic consistencies. The results observed here corroborate previous studies, which show the conservative nature of sperm morphology. However, ultrastructural character combinations specific to sperm and spermiogenesis seem to differ among taxa. Further studies into sperm morphology are needed in order to judge the relevance of the ontogenic changes recorded here and to determine their role in future studies on amniote evolution.

1. Introduction

An extensive review of the reproductive literature within the last decade reveals an accumulation of ultrastructural studies detailing the morphology of mature spermatozoa (e.g. Teixeira et al., 2002; Vieira et al., 2004, 2005; Tourmente et al., 2008; Röll and von Düring, 2008) in the Lepidosauria (Squamata + Sphenodontida). In contrast, few manuscripts have focused on the ontogenic steps of spermiogenesis within reptiles. Spermiogenesis is the step-wise development of spermatids into the mature spermatozoa, and many of the characters observed in mature spermatozoa are seen throughout this developmental process. Useful non-traditional characters developed from the ultrastructure of the mature spermatozoa have previously been used in phylogenetic analyses (Jamieson, 1991, 1995, 1999; Newton and Trauth, 1992; Jamieson et al., 1996; Gribbins and Rheubert, in press), many of which have found sperm characters to be highly conserved among reptilian taxa (Teixeira et al., 1999a,b; Gribbins and Rheubert, in press). Since the developmental characters of spermiogenesis often disclose the final morphological details of the mature spermatozoa (Gribbins et al., 2007, 2010; Rheubert et al., 2010c), equal focus on spermiogenesis may add to the robustness of these phylogenetic analyses by providing novel ontogenic characters.

Ultimately, recent ultrastructural analyses that infer evolutionary trends among reptiles have shown that some spermatozoa morphology characters may be synapomporphic among squamates. For example, Jamieson (1995) found that a single perforatorium may be a synapomorphy for squamates in their study of Iguania, and Jamieson (1999), Vieira et al. (2004), and Rheubert et al. (2010a) corroborated these data in their analysis in the within the Squamata. Also, the peripheral fibers associated with microtubule doublets 3 and 8 are grossly enlarged in squamates (Jamieson, 1995, 1999; Cunha et al., 2008), whereas in *Sphenodon* they are not (Healy and Jamieson, 1992). However, with very few taxa of squamates having been examined morphologically, these data are extremely preliminary until future studies either add more information on the known ultrastructural data or new taxa are examined.

* Corresponding author.
E-mail address: Justin.rheubert@selu.edu (J.L. Rheubert).

0968-4328/$ – see front matter © 2011 Elsevier Ltd. All rights reserved.
doi:10.1016/j.micron.2011.03.006

Lepidosaurs have largely been ignored in terms of describing the complete steps of spermiogenesis although many previous studies regarding sperm development in reptiles focused on specific steps or details of spermiogenesis (i.e., acrosome development, nuclear condensation/elongation, and flagellar development) (Clark, 1967; Butler and Gabri, 1984; Hondo et al., 1994; Al-Dokhi, 2004, 2009; Mubarak, 2006). To date, only seven studies provide comprehensive descriptions of spermiogenesis in Lepidosaurs: *Chalcides ocellatus* (Carcupino et al., 1989), *Sphenodon punctatus* (Healy and Jamieson, 1994), *Tropidurus torquatus* (Vieira et al., 2001), *Iguana iguana* (Ferreira and Dolder, 2002), *Scincella lateralis* (Gribbins et al., 2007), *Agkistrodon piscivorus* (Gribbins et al., 2010), and *Anolis lineatopus* (Rheubert et al., 2010c). These studies have shown that the major events associated with spermiogenesis follow general patterns although specific ultrastructural differences exists, such as presence/absence of a manchette, endoplasmic reticulum involvement in acrosome development, number and composition of acrosomal layers, and location of the acrosome granule upon first appearance. These studies also reveal that many, if not all, of the characters used in evolutionary analyses of mature spermatozoa become apparent during the stages of spermiogenesis.

Presently, few studies exist on the mature spermatozoa of geckos (Furieri, 1970; Jamieson et al., 1996; Röll and von Düring, 2008); however, no studies highlight the ultrastructure of spermiogenesis within the Gekkonidae (senus stricto, excluding pygopods), a cosmopolitan family of over 1000 named species (Han et al., 2004). Thus, the purpose of this study is to describe the events of spermiogenesis within the Mediterranean Gecko, *Hemidactylus turcicus*. The results from this study will be compared to the mature sperm of geckos and to what is known about spermiogenesis in other squamates. This is the fifth study on reproductive morphological characters in *H. turcicus*, which include female sperm storage (Eckstut et al., 2009), germ cell development (Rheubert et al., 2009), testicular duct morphology (Rheubert et al., 2010b), and sexual segment morphology (Rheubert et al., 2010a).

2. Materials and methods

2.1. Tissue collection

Sexually mature male geckos were collected from March 2006 to March 2009 in Hammond, LA, and euthanized by means of a 0.2 cc intraperitoneal injection of sodium pentobarbitol as approved by the Animal Care and Use Committee at Southeastern Louisiana University. Specimens were dissected and tissues were submerged in Trump's Fixative (EMS, Hatfield, PA) for at least 24 h. Tissues from the above collection were selected from pre-determined spermiogenically active months (June, July, and August; $n = 6$) (Rheubert et al., 2009) to be used in this study.

2.2. Tissue preparation for electron microscopy

Testicular tissues fixed in Trump's solution were rinsed with deionized water, post-fixed in 2% osmium tetroxide, and dehydrated in a graded series of ethanol solutions. Tissues were then cleared with propylene oxide, infiltrated with a 1:1 solution of propylene

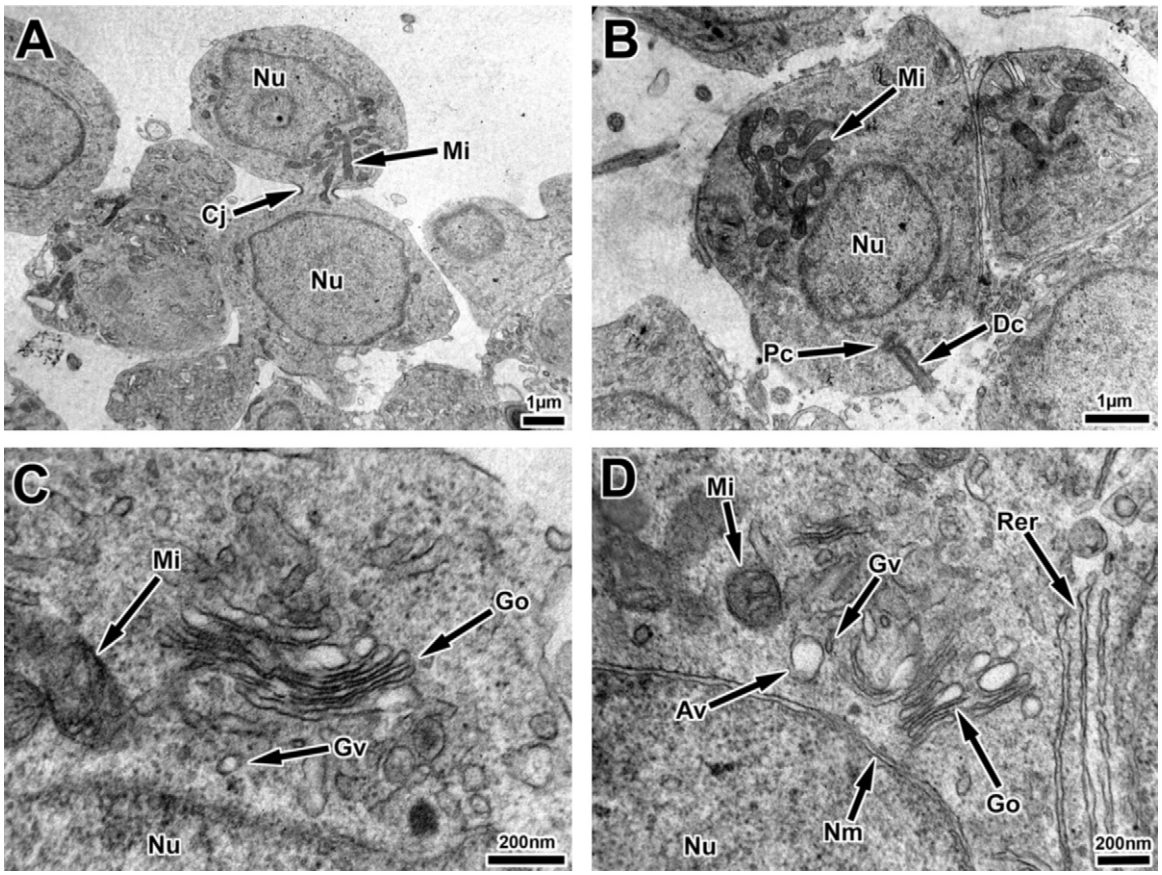

Fig. 1. Early stages of spermiogenesis within the seminiferous epithelium of *H. turcicus*. (A) Germ cells are connected by cytoplasmic junctions (Cj) and organelles such as mitochondria (Mi) are shared between cells. Nucleus (Nu). (B) Early stage of spermiogenesis depicting the grouping of mitochondria (Mi) apical to the nucleus (Nu). The proximal (Pc) and distal (Dc) centrioles can be seen arranged perpendicular to one another at the posterior edge of the germ cell. (C) The beginning stages of acrosome development involve a supranuclear Golgi complex (Go) with budding Golgi vesicles (Gv). Mitochondria (Mi) are also observed in their position apical to the nucleus (Nu). (D) Golgi vesicles (Gv) budding from the Golgi complex (Go) converge apical to the nucleus (Nu) beginning the formation of the acrosomal vesicle (Av) which does not make contact with the nuclear membrane (Nm). Rough endoplasmic reticulum (Rer) and mitochondria (Mi) are also observed at the apical portion of the germ cell.

oxide:epoxy resin, 1:2 solution of propylene oxide:epoxy resin, and then placed in 100% epoxy resin for 36 h under vacuum. Samples were embedded in fresh epoxy resin and cured at 60 °C for 48 h.

2.2.1. Microscopy

Dry glass knives and an LKB microtome (LKB Produkter AB, Bromma, Sweden) were used to face tissue blocks before thin sections (90 nm) were taken using a Leica EM UC7 ultramicrotome (Leica Microsystems, Vienna Italy) and a diamond knife (Diatome, Hatfield, PA). Sections were placed on 300 mesh copper grids, stained with uranyl acetate and lead citrate, and viewed with a JEOL JEM-1200 EXII transmission electron microscope (Jeol Inc., USA). Representative photographs of different stages of spermiogenesis were taken using a Gatan 785 Erlangshen digital camera (Gatan Inc., Warrendale, PA). Composite micrographs were constructed using Adobe Photoshop CS5 (Adobe Systems, San Jose, CA).

3. Results

Spermatids entering the initial stages of spermiogenesis are joined by cytoplasmic bridges (Fig. 1A, Cj), which allow for cellular communication and sharing of organelles such as mitochondria (Fig. 1A, Mi) during early development. Flagellar development is one of the first processes to begin in round spermatids with the proximal centriole (Fig. 1B, Pc) and distal centriole (Fig. 1B, Dc) lining up perpendicular to one another and the distal centriole starting elongation. Mitochondria (Fig. 1B, Mi) become concentrated within the apical cytoplasm in proximity to where acrosome development will commence. A prominent Golgi complex (Fig. 1C and D, Go) becomes evident in the perinuclear region. The Golgi complex is swollen in appearance and multiple vesicles (Fig. 1C and D, Gv) bud from the cis cisternum of the Golgi complex. Transport vesicles that arise from the Golgi merge near the apical aspect of the nucleus (Fig. 1C and D, Nu) forming the early acrosomal vesicle (Fig. 1D, Av). The acrosomal vesicle at this point does not make contact with the nuclear membrane (Fig. 1D, Nm). Mitochondria (Fig. 1C and D, Mi) and rough endoplasmic reticulum (Fig. 1D, Rer) are also evident in the perinuclear region.

Transport vesicles (Fig. 2A, Gv) continue to merge with the acrosomal vesicle (Fig. 2A, Av), which increases in size causing a slight indentation in the apex of the nucleus (Fig. 2A, Nu). The contents of the transport vesicles are released into the growing acrosomal vesicle (Fig. 2A and B, Av) and intra-acrosomal vesicles (Fig. 2B, Iv) form inside the acrosomal vesicle during the early round spermatid stage. The acrosomal vesicle remains detached from the nucleus and a prominent subacrosomal space (Fig. 2A, Sas) is observed between the membranes of the acrosome and nucleus. The cytoplasm begins to shift causing mitochondria (Fig. 2A, Mi) and rough endoplasmic reticulum (Fig. 2A, Rer) to migrate towards the basal portion of the cell. The proximal centriole (Fig. 2C, Pc) and distal centriole become more developed and the distal centriole continues to elongate forming the growing axoneme of the flagellum (Fig. 2C, Ef). An indentation at the posterior nucleus (Fig. 2D, Nu) forms the nuclear fossa (Fig. 2D, Nf).

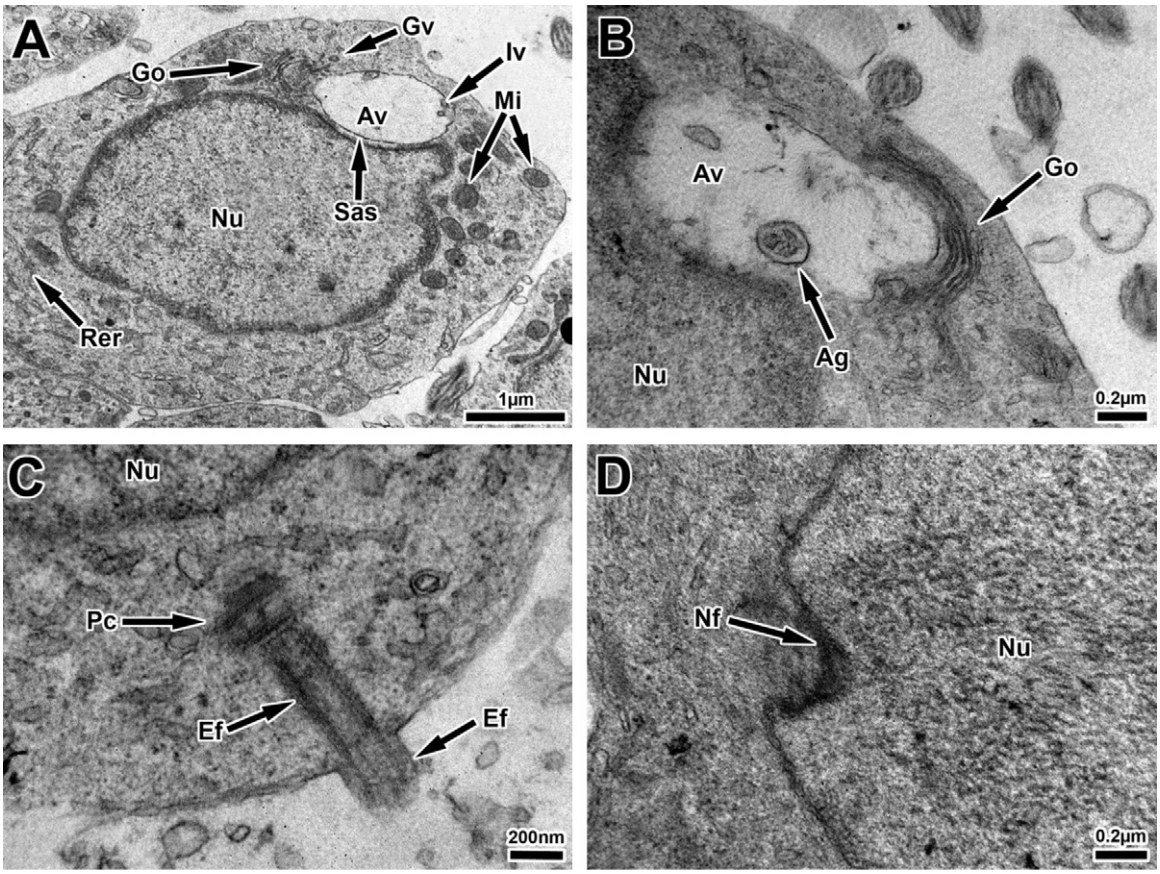

Fig. 2. Continuing developmental stages early in spermiogenesis. (A) Golgi vesicles (Gv) budding from the Golgi complex (Go) continue to converge causing the acrosomal vesicle (Av) to increase in size. An indentation is formed at the apical aspect of the nucleus (Nu) but the acrosomal vesicle does not make contact with the nucleus beginning the development of the subacrosomal space (Sas). Mitochondria (Mi) and rough endoplasmic reticulum (Rer) can be seen migrating posteriorly during the cytoplasmic shift. (B) Activity of the Golgi complex (Go) decreases as the acrosome vesicle (Av) approaches its final size. A dense body can be seen migrating to the posterior portion of the acrosome vesicle where it will become the acrosome granule (Ag). Nucleus (Nu). (C) The proximal (Pc) and distal centriole can be seen posterior to the nucleus (Nu). The distal centriole begins its development as the elongating flagellum (Ef). (D) An indentation at the posterior portion of the nucleus (Nu) forms the nuclear fossa (Nf) where the proximal centriole will be situated.

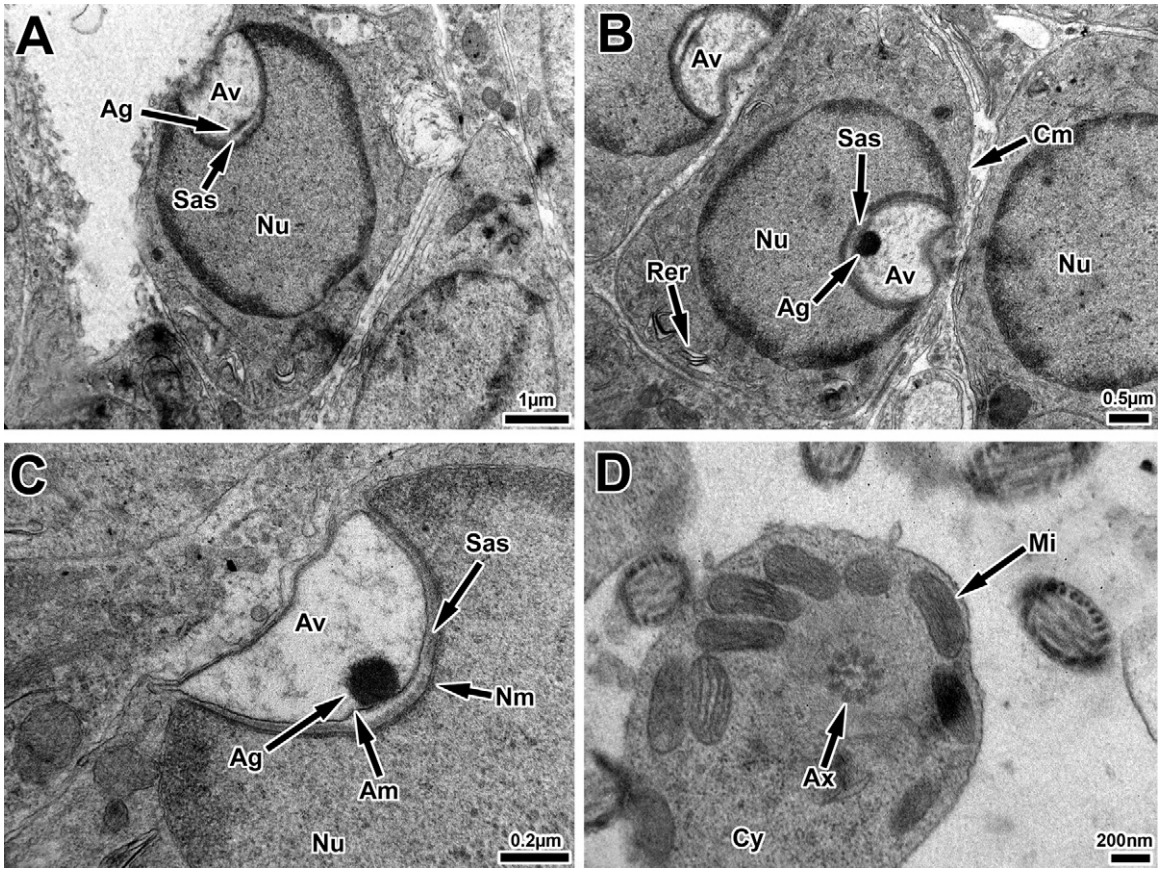

Fig. 3. Early stages of elongation during spermiogensis. (A) The indentation at the apical portion of the nucleus (Nu) caused by the acrosome vesicle (Av) continues to increase. The acrosome granule (Ag) can be seen fully condensed in its basal position. The formation of the subacrosomal space (Sas) continues as the chromatin begins to condense at the borders of the nucleus. (B) As the acrosome vesicle (Av) creates a larger indentation at the apical portion of the nucleus (Nu) the cytoplasm begins to rearrange with more cytoplasm accumulating in the posterior region taking organelles such as rough endoplasmic reticulum (Rer) with it. The developing germ cells stay in close association with one another. Acrosomal granule (Ag), subacrosomal space (Sas), and cell membrane (Cm). (C) Development of the subacrosomal space (Sas) continues and a band of proteins can be observed between the nuclear membrane (Nm) and the membrane (Am) of the acrosome vesicle (Av). The acrosomal granule (Ag) is fully condensed in its basal position. Nucleus (Nu). (D) Mitochondria (Mi) begin to arrange themselves around the axoneme (Ax) of the distal centriole as the cytoplasm (Cy) continues to shift towards the posterior end of the germ cell.

Acrosome formation is completed when vesicle production from the Golgi complex terminates and the acrosomal vesicle (Fig. 3A, B and C, Av) has reached its final size prior to elongation. A round acrosomal granule is set basally in the acrosome, which resides in a deep depression within the apical nucleus (Fig. 3A, Ag, Nu). The acrosomal granule (Fig. 3B and C, Ag) rests on the inner acrosomal membrane (Fig. 3C, Am). Protein accumulation continues between the nuclear membrane (Fig. 3C, Nm) and acrosomal membrane (Fig. 3C, Am) within the subacrosomal space (Fig. 3B and C, Sas). At the end of acrosome formation, the round spermatid nucleus occupies the most apical portion of the cell directly adjacent to the cell membrane (Fig. 3B, Cm) with minimal cytoplasm in this region. The cytoplasm and organelles are pushed to the posterior portion of the cell and mitochondria migrate to the cytoplasm (Fig. 3D, Cy) surrounding the axoneme (Fig. 3D, Ax) of the distal centriole.

Round spermatids then enter the elongation and condensation phase of spermiogenesis. The chromatin of the nucleus (Fig. 4A and B, Nu) begins to condense in a slightly spiral and granular fashion during early elongation. The developing spermatid nucleus continues to push against the cell membrane (Fig. 4A, Cm) causing the acrosomal vesicle (Fig. 4A, Av) and acrosomal granule (Fig. 4A, Ag) to flatten against the apex of the nucleus leaving the subacrosomal space (Fig. 4A, Sas) intact. As the chromatin condenses the germ cell elongates and both longitudinal microtubules (Fig. 4B, Lmm) and circum-cylindrical microtubules (Fig. 4B, Cmm), which make up the manchette, are evident. The organelles become concentrated in the posterior portion of the cytoplasm with the rough endoplasmic reticulum (Fig. 4C, Rer) in close association with the anlage of the annulus (Fig. 4C, An). The future site of the midpiece of the flagellum continues to develop as it becomes fully encircled by mitochondria (Fig. 4D, Mi) and the fibrous sheath of the principal piece (Fig. 4D, Fs) becomes evident.

Nuclear condensation and elongation continues as the nucleus (Fig. 5A, B and C, Nu) becomes more electron-dense and more cylindrical in shape. The acrosomal vesicle (Fig. 5A and B, Av) begins to envelop the head of the nucleus by migrating laterally along the peripheral edges of the nuclear apex, although a majority of the acrosome complex remains in the apical position. The acrosomal granule becomes more diffuse (Fig. 5A, Ag) but remains in contact with the inner acrosomal membrane. The acrosome complex appears to have emerged from the cytoplasm of the germ cell (Fig. 5A) as the amount of cytoplasm between the cell membrane and acrosome becomes depleted. The result of the acrosome and cell membranes merging together gives the acrosome complex an electron-dense appearance (Fig. 5A and B, Av). The nuclear fossa (Fig. 5C, Nf) remains intact and two electron lucent nuclear shoulders (Fig. 5B and C, Ns) surround the nuclear fossa. The flagellum (Fig. 5B, C and D, Fl) extends away from the germ cell proper and is surrounded by Sertoli cells (Fig. 5D, Scm) near its base during this point of spermiogenesis. The Sertoli cell contains multiple mitochondria (Fig. 5D, Mi) and an extensive rough endoplasmic reticulum (Fig. 5D, Rer).

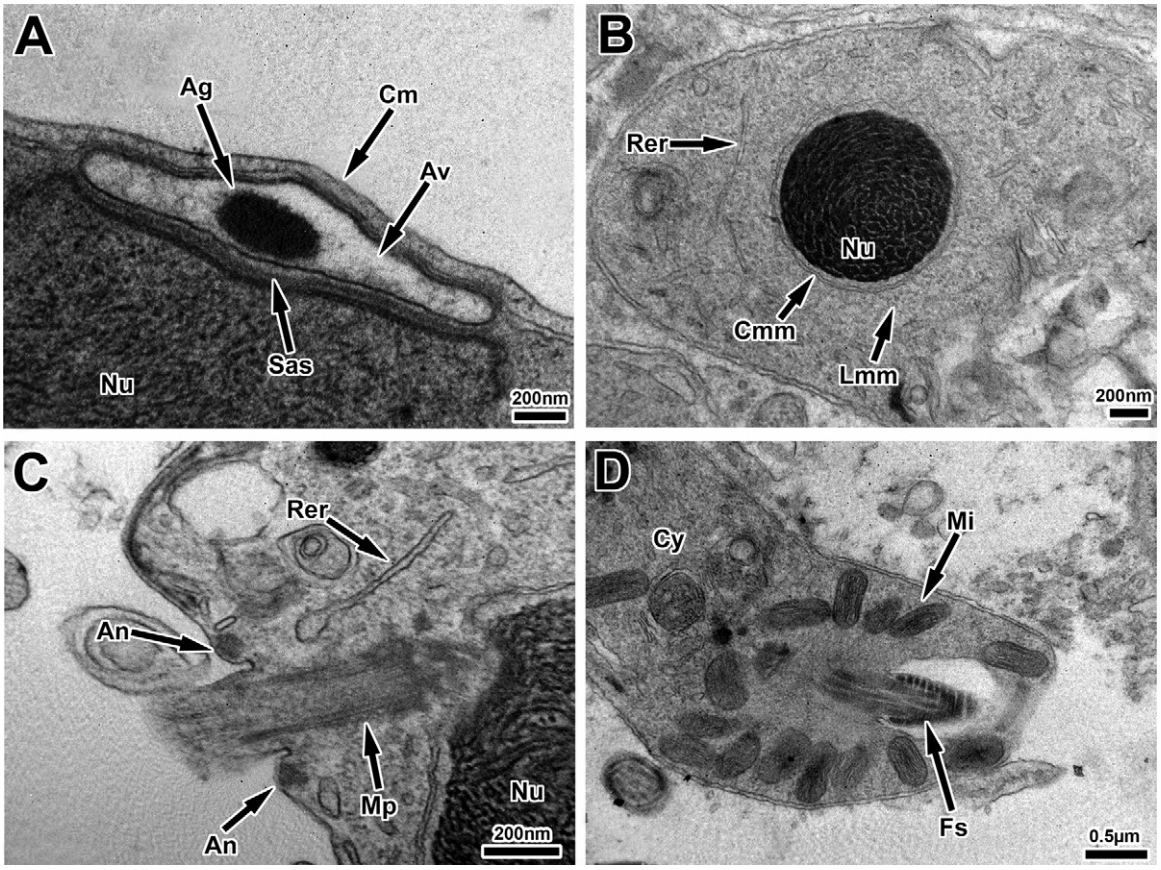

Fig. 4. Continuing stages of elongation during spermiogenesis. (A) During the cytoplasmic shift the cell membrane (Cm) pushes on the apical portion of the germ cell causing the acrosomal vesicle (Av) and acrosomal granule (Ag) to flatten against the nucleus (Nu). However, the subacrosomal space (Sas) remains between the acrosome vesicle and the nucleus. (B) The chromatin within the nucleus (Nu) begins to condense in a slightly spiral fashion. Both longitudinal (Lmm) and circumcylindrical (Cmm) microtubules of the manchette can be seen. Rough endoplasmic reticulum (Rer). (C) Posterior to the nucleus (Nu) the midpiece (Mp) of the flagellum can be seen within the cytoplasm. Rough endoplasmic reticulum (Rer) is seen in close association with the developing annulus (An). (D) As the flagellum elongated the development of the fibrous sheath (Fs) can be observed. Mitochondria (Mi) continue to migrate within the cytoplasm (Cy) to their final destination at the midpiece.

At the climax of nuclear elongation and condensation the acrosome is surrounded by multiple Sertoli cell processes, particularly towards the head of the developing spermatid. Rough endoplasmic reticulum (Fig. 6A, Rer) is observed within the surrounding Sertoli cell processes, juxtapositioned to the acrosome complex. The acrosomal vesicle becomes partitioned into the outer acrosomal cortex (Fig. 6A, Aco) and the inner, more electron-dense, acrosomal medulla (Acm). The perforatorium (Fig. 6A, Perf) extends into the acrosomal cortex and the perforatorial base plate (Fig. 6A, Pbp) begins to develop as a central densification of the apical portion of the subacrosomal space. The nucleus (Fig. 6B, C and D, Nu) is homogenous in electron density and fully enveloped by the microtubules of the manchette (Fig. 6B, Lmm). Mitochondria (Fig. 6C, Mi) are concentrated in a basal position within the germ cell near the caudal end of the nucleus (Fig. 6C, Nu). Dense bodies (Fig. 6C inset, black arrowhead) separate the individual mitochondria (Fig. 6C inset, Mi). The proximal centriole (Fig. 6C and D, Pc) resides within the nuclear fossa (Fig. 6C and D, Nf) and is almost perpendicular to the distal centriole (Fig. 6D, Dc) at a final angle of approximately 80°. Thickening of the connecting piece (Fig. 6D, Cp) forms the link between the proximal centriole and flagellar components.

Prior to completing spermiogenesis much of the cytoplasmic material of the developing germ cell is shed and the spermatid becomes enveloped by multiple Sertoli cell processes. A single Sertoli cell (Fig. 7A, Sc1) surrounds the acrosomal complex and nucleus (Fig. 7C, Nu) of the developing germ cell. This Sertoli cell is electron lucent, contains cisternae of smooth endoplasmic reticulum (Fig. 7A and C, Er), and displays properties of ectoplasmic specializations (Fig. 7C, white arrowheads). A second Sertoli cell (Fig. 7A and B, Sc2) surrounds the electron lucent Sertoli cell. The outer Sertoli cell is electron-dense and contains organelles such as mitochondria (Fig. 7A and B, Mi). This wrapping of Sertoli cells gives the appearance of multiple membranes (Fig. 7C, Sc1m and Sc2m) around a developing spermatid where the acrosomal membrane, germ cell membrane, and Sertoli cell membranes can all be observed in cross-section. Flagellar development culminates with mitochondria (Fig. 7D, Mi) and dense bodies (Fig. 7D, Db) surrounding the fibrous sheath (Fig. 7D, Fs) within the midpiece. The midpiece terminal is marked by the electron-dense annulus (Fig. 7D, An).

Many of the characteristics observed in the mature spermatozoa become evident during the final stage of spermiogenesis. The acrosome complex is circular in cross section and highly compartmentalized with an electron-dense acrosomal cap (Fig. 8A, B and C, Acc) surrounding the acrosome complex. The acrosome is divided into an outer electron lucent cortex (Fig. 7A, B and D, Aco) and inner electron-dense medulla (Fig. 8A and B, Acm). A single perforatorium (Fig. 8A and B, Perf) with a round tip extends up into the acrosome and rests on a stopper-like basal plate within the subacrosomal space (Fig. 8A, Pbp, Sas). An elongation of the apical nucleus (Fig. 7A and D, Nu), known as the nuclear rostrum (Fig. 8A, Nr), extends into the subacrosomal space (Fig. 8A and D, Sas) and is capped by an epinuclear lucent zone (Fig. 8A and C, Enc). The nucleus (Fig. 8E, Nu) is homogenous in electron density and devoid of any lacunae. Both longitudinal microtubules (Fig. 8E, Lmm) and circum-cylindrical microtubules (Fig. 8E, Cmm) of the manchette surround the nucleus (Fig. 8E, Nu).

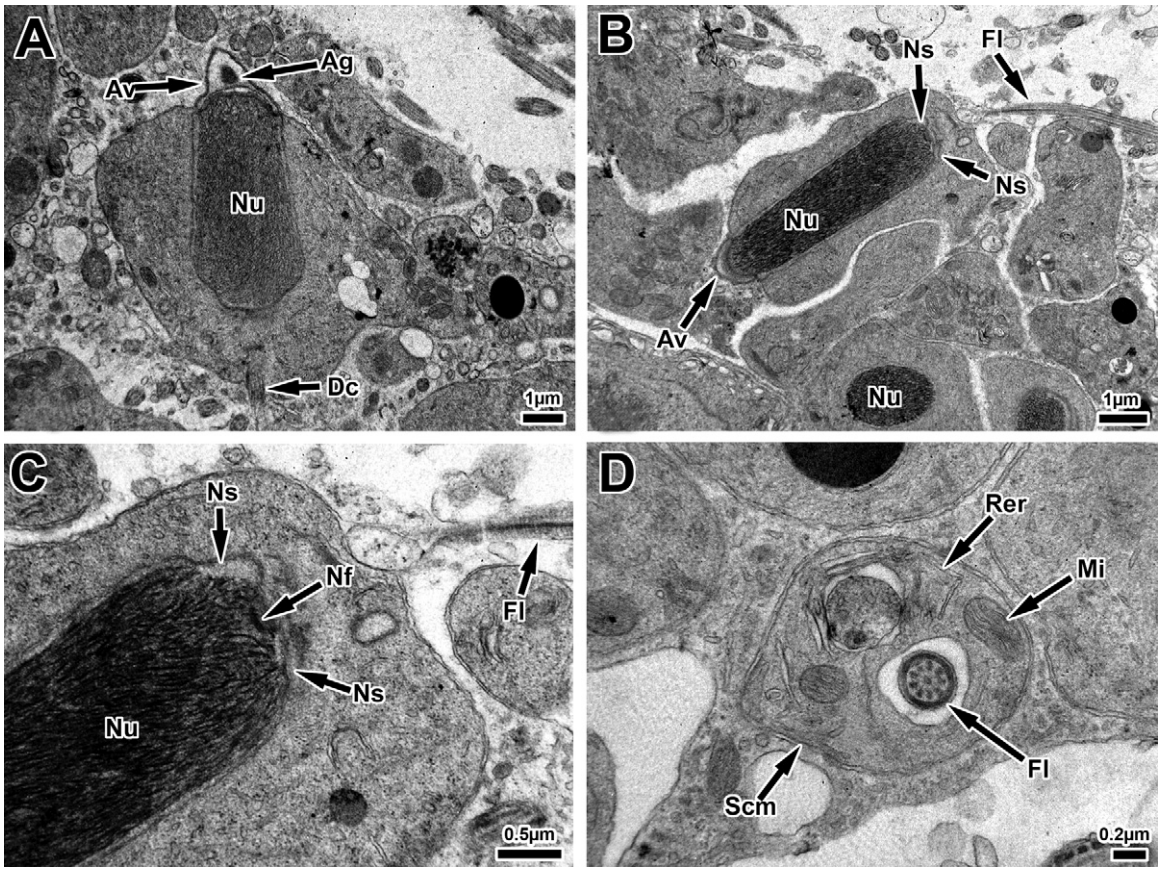

Fig. 5. Continuing stages of elongation during spermiogenesis. (A) As the acrosome becomes devoid of cytoplasm and begins to envelop the nucleus (Nu) the majority of the acrosomal vesicle (Av) and acrosomal granule (Ag) lie apical to the nucleus. Distal centriole (Dc). (B) The nucleus (Nu) continues to elongate as the acrosome vesicle (Av) begins to envelop the nucleus and becomes devoid of cytoplasm. Electron lucent nuclear shoulders (Ns) can be seen juxtapositioned to the nuclear fossa. Flagellum (Fl). (C) As the nucleus (Nu) continues elongation and chromatin condensation the electron lucent shoulders (Ns) become prominent juxtapositioned to the nuclear fossa (Nf). Flagellum (Fl). (D) The flagellum (Fl) extends exterior to the germ cell cytoplasm and becomes associated with Sertoli cells (Scm). The Sertoli cell is filled with mitochondria (Mi) and rough endoplasmic reticulum (Rer).

The flagellum is divided into the connecting piece (Fig. 9A, Cp), midpiece (Fig. 9A, Mp), principal piece (Fig. 9A, Pp), and endpiece (Fig. 9A, Ep). The connecting piece displays a 9+3 microtubule arrangement in cross section (Fig. 9B, 9+3) with outer fibers (Fig. 9B, Of) associated with each microtubule triplet. An outer ring of proteins (Fig. 9B, Pr) surrounds the microtubule arrangement and a ring of mitochondria (Fig. 9C, Mi) and dense bodies (Fig. 9C, Db) surround the beginning of the axoneme (Fig. 9C, Ax) of the midpiece. The mitochondrial ring continues into the midpiece (Fig. 9A;D Mi) with dense bodies (Fig. 9A and D, Db) separating the mitochondria. The mitochondria (Fig. 9D, Mi) contain linear cristae and appear ovoid in cross-section and columnar in sagittal section (Fig. 9A, Mi). A fibrous sheath (Fig. 9A and D, Fs) surrounds the axonemes of the caudal portion of the connecting, mid, and principal pieces and the peripheral fibers (Fig. 9D, Pf) associated with microtubule doublets 3 and 8 are grossly enlarged in the midpiece only. The midpiece terminates at the annulus (Fig. 9A, An) but the fibrous sheath (Fig. 9A and E, Fs) continues into the principal piece (Fig. 9, Pp). The peripheral fibers associated with microtubule doublets 3 and 8 are not enlarged in the principal piece. The fibrous sheath terminates at the beginning of the endpiece (Fig. 9, Ep) where the axoneme (Fig. 9F, Ax) is considered naked or uncovered (Fig. 9F, Dc).

4. Discussion

Spermiogenesis within the testis of *H. turcicus* follows the same general steps as other Lepidosaurian species studied to date (i.e., acrosome formation, nuclear elongation/chromatin condensation, flagellar development) and thus allows for comparative studies of spermatid morphology among reptilian groups and other vertebrate taxa (Russell et al., 1990; Healy and Jamieson, 1994; Ferreira and Dolder, 2002; Gribbins et al., 2007). These developmental characters lead to the characters seen in mature spermatozoa. Rheubert et al. (2010a) showed, in the spermatozoon of snakes, many of the characters are conserved. Results from their study suggest the acrosome complex is highly conserved, and much of the variation in sperm morphology is observed within the flagellum.

During spermatid development the acrosome becomes highly compartmentalized and contains groups of proteins and hydrolytic enzymes (Talbot, 1991) that aid in fertilization. In *H. turcicus* the acrosome complex consists of an acrosomal cap, cortex, medulla, perforatorium, and subacrosomal cone. A single perforatorium, proposed as a synapomorphy for squamates (Teixeira et al., 1999b; Tavares-Bastos et al., 2007; Tourmente et al., 2008), also protrudes into the subacrosomal space of late elongating spermatids in *H. turcicus*. It is during spermiogenesis that this compartmentalization becomes apparent through processes similar to that of other amniotic spermatids and spermatozoa studied to date.

Vesicles from the Golgi complex in *H. turcicus* fuse with the acrosome vesicle causing it to increase in size. Ferreira and Dolder (2002) suggested that the endoplasmic reticulum aids in the development of the acrosome complex in *I. iguana*, but development of the acrosome in *H. turcicus* and all other squamates studied to date occurs through the fusion of vesicles arising from the Golgi complex. Throughout acrosome development in *H. turcicus*, rough

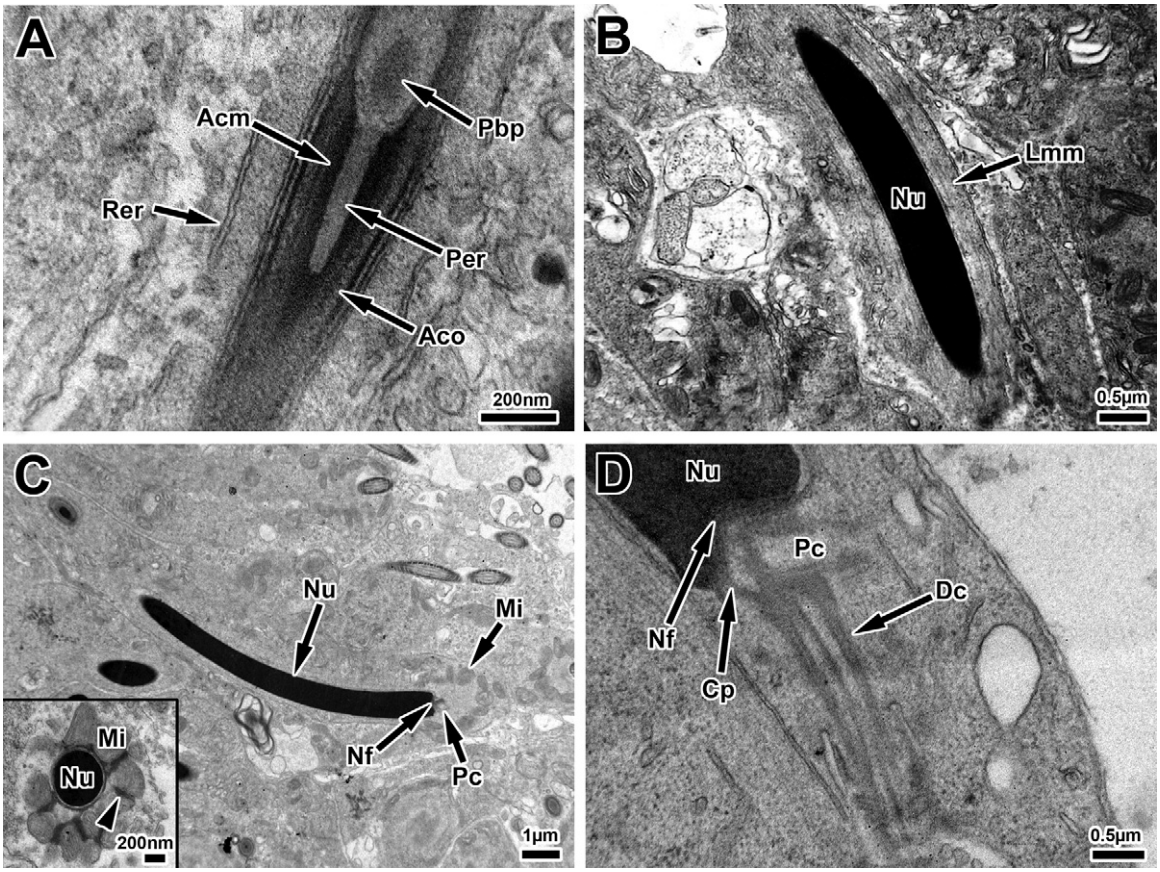

Fig. 6. Late elongation of the germ cell during spermiogenesis. (A) The acrosome becomes highly compartmentalized containing a cortex (Aco) and medulla (Acm). Within the medulla the perforatorium (Per) and perforatorial base plate (Pbp) can be observed. Rough endoplasmic reticulum (Rer) is observed in the surrounding Sertoli cell. (B) Late in elongation the nucleus (Nu) becomes homogenous in electron density and the microtubules of the manchette (Lmm) can be observed. (C) The proximal centriole (Pc) is situated in the nuclear fossa (Nf) at the posterior portion of the nucleus (Nu). The mitochondria (Mi) have almost reached their final destination surrounding the midpice. Inset: Mitochondria (Mi) continue to migrate posterior to the nucleus (Nu) and dense bodies (black arrowhead) are observed between the mitochondria. (D) At the posterior portion of the nucleus (Nu) the proximal centriole (Pc) is situated in the nuclear fossa (Nf). The distal centriole (Dc) is connected to the proximal centriole (Pc) via the connecting piece (Cp).

endoplasmic reticula are located juxtapositioned to the Golgi complex, but the endoplasmic reticulum is not directly involved in acrosome formation. Intrinsic vesicles found within the acrosome may originate from the endoplasmic reticulum and Healy and Jamieson (1994) suggested these intrinsic vesicles were being exocytosed from the acrosome in *S. punctatus*. Moreno et al. (2000) corroborated their data using molecular signaling in Rhesus monkeys (*Macaca mulatta*), stating that proteins from the endoplasmic reticulum transported by the Golgi complex may end up in the wrong destination (the acrosome) only to be returned to the Golgi by Clathrin and β-COP1-coated vesicles.

Protein stratification observed within the subacrosomal space observed in *A. lineatopus* (Rheubert et al., 2010c) and the snake, *A. piscivorus* (Gribbins et al., 2010) was not seen in *H. turcicus*. The subacrosome space in the Mediterranean Gecko is uniformly paracrystalline with a single perforatorium, which is proposed to develop from the acrosome granule (Del Conte, 1976), extending into the subacrosomal cone similar to that of other squamates (Tourmente et al., 2008). This microtubule composite structure rests on a perforatorial basal plate, which also is present in all non-scincomorphs studied to date except *Bradypodion karrooicum* (Jamieson, 1995), *Tropidurus semitaeniatus*, and *T. torquatus* (Teixeira et al., 1999a).

The acrosome granule of the Mediterranean Gecko is first observed in a basal location similar to other lizard species except *S. lateralis*, in which the granule is seen before the vesicle approaches the nuclear membrane. As seen in *A. lineatopus* (Rheubert et al., 2010c) the acrosome granule flattens as the acrosome vesicle begins to envelop the nucleus. During this developmental time the cytoplasm is pushed to the posterior portion of the germ cell and organelles migrate to the base of the nucleus comparable to that observed in other squamates. During these early stages the centrioles of the flagellum become evident posteriorly to the caudal end of the nucleus and are positioned at approximately 80° within the nuclear fossa. Multiple cytoplasmic bridges remain intact between spermatids similar to that in other squamates (Ferreira and Dolder, 2003; Gribbins et al., 2007). However, our study actually provides visual evidence that organelles are shared between germ cells through these intercellular connections further suggesting cellular communication (Jamieson, 1981; Ventela et al., 2003), which may allow germ cells to develop as a single cohort throughout development within reptiles as proposed by Gribbins and Gist (2003).

During the elongation phases of spermiogenesis, the nucleus begins to lengthen along its antero-posterior axis, which is aided by microtubules of the manchette. The microtubules of the manchette have been observed in all squamates studied to date with the exception of *A. lineatopus* (Rheubert et al., 2010c). This process gives rise to the cylindrical shape of the mature spermatozoon observed in other amniotes (Jamieson, 1991). The chromatin condenses in a slightly spiraling fashion similar to that of *I. iguana* (Ferreira and Dolder, 2002) and *A. piscivorus* (Gribbins et al., 2010). This differs from the granular condensation of *A. lineatopus* (Rheubert

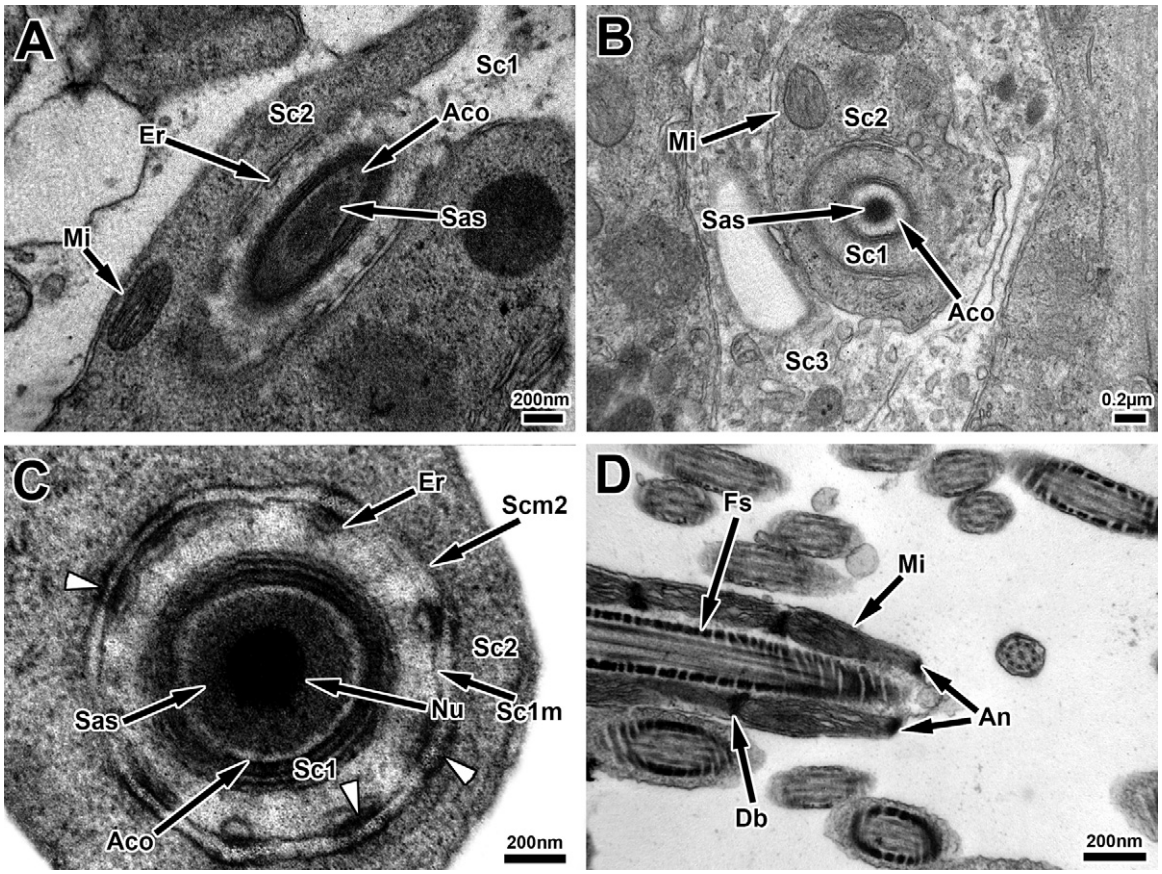

Fig. 7. Late stages of the germ cell elongation during spermiogenesis. (A) Cross-sectional view through a late elongate acrosome detailing the inner subacrosomal space (Sas) and outer acrosomal cortex (Aco). Surrounding the acrosomal cap is the inner Sertoli cell (Sc1) that contains coated vesicles (Cv) and exhibits ectoplasmic specializations (Es). An outer Sertoli cell (Sc2) encompasses portions of the inner Sertoli cell and contains cellular organelles such as mitochondria (Mi). (B) Cross-section view through the subacrosome space (Sas) and surrounding acrosome cortex(Aco) shows 3 Sertoli cells (Sc) associated with a single germ cell. Mitochondria (Mi). (C) High power cross-sectional view of a late elongate nuclear rostrum (Nu). The nucleus is surrounded by the subacrosome space (Sas) and acrosomal cortex (Aco). Associated Sertoli cells (Sc1, Sc2) and their membranes (Sc1m, Sc2m) are observed. Smooth endoplasmic reticulum (Er) and ectoplasmic specializations (white arrowheads) are also observed. (D) Sagittal section through the posterior end of the midpiece detailing fibrous sheath (Fs), and surrounding mitochondria (Mi) and dense bodies (Db). The midpiece terminates at the annulus (An).

et al., 2010c) and *S. lateralis* (Gribbins et al., 2007). Throughout the process of nuclear elongation and acrosome envelopment in *H. turcicus* a small portion of the nucleus, termed the nuclear rostrum (Clark, 1967) extends into the subacrosomal cone and is capped by an epinuclear lucent zone, which is absent in *Heteronotia binoei* (Jamieson et al., 1996), present in *Lygodactylus picturatus* and *Hemidactylus frenatus* (Furieri, 1970), and present during development in *A. lineatopus* (Rheubert et al., 2010c). At the basal portion of the nucleus two electron lucent shoulders surrounding the nuclear fossa become visible in *H. turcicus* which is also noticed during the maturation in *A. piscivorus* (Gribbins et al., 2010).

As flagellar development in *H. turcicus* continues the distal centriole within the connecting piece degrades, similar to that observed in others amniotes (Fawcett, 1970), and the microtubule triplets (9 + 3 arrangement) persists. The distal centriole elongates and displays the conserved 9 + 2 microtubule arrangement. The fibrous sheath of late elongating spermatids within the Mediterranean Gecko surrounds the axoneme beginning at mitochondrial tier 3 similar to that of some teiids (*Tupinambis merianae*, Tavares-Bastos et al., 2002; *Crocodilurus amazonicus*, Colli et al., 2007; *Draceana guianensis*, Colli et al., 2007). However, in other gekkonids the fibrous sheath is observed beginning at mitochondrial tier 2 (Furieri, 1970). Mitochondria of *H. turcicus* also surround the midpiece, which terminates at an irregular shaped annulus. The annulus is proposed to keep the mitochondria in close association with the axoneme during flagellar oscillation and seen within all amniotic spermatozoa (Fawcett, 1970). Within the midpiece the dense fibers associated with microtubule doublets 3 and 8 are grossly enlarged similar to all other squamates (Jamieson, 1995, 1999; Rheubert et al., 2010a) but differing from *S. punctatus*, which lacks these enlargements (Healy and Jamieson, 1994). The lack of surrounding mitochondria and grossly enlarged fibers at doublets 3 and 8 mark the beginning of the principal piece in *H.* turcicus and is similar to *H. binoei* (Jamieson et al., 1996). However, in several squamate species the dense fibers at microtubule doublets 3 and 8 remain enlarged in the principal piece (*Laenaetus longipes*, Vieira et al., 2004; *Oplurus cyclurus*, Vieira et al., 2007; *Tropidurus itambere*; Ferreira and Dolder, 2003).

Throughout sperm development in *H. turcicus* a close association between germ cells and surrounding Sertoli cells is observed. Sertoli cells are often referred to as nurse cells because of their intimate association with developing germ cells, which leads to the formation of a variety of cellular junctional complexes. Sertoli cells frequently form interdigitating tight junctions between one another and the juxtapositioned germ cells (Russell et al., 1990). These tight junctions also accumulate concentrated actin bundles and associated endoplasmic reticulum to form a cell membrane related complex known as an ectoplasmic specialization (Mruk et al., 2008). These sustentacular cells are situated within the seminiferous epithelium with multiple cellular extensions allowing

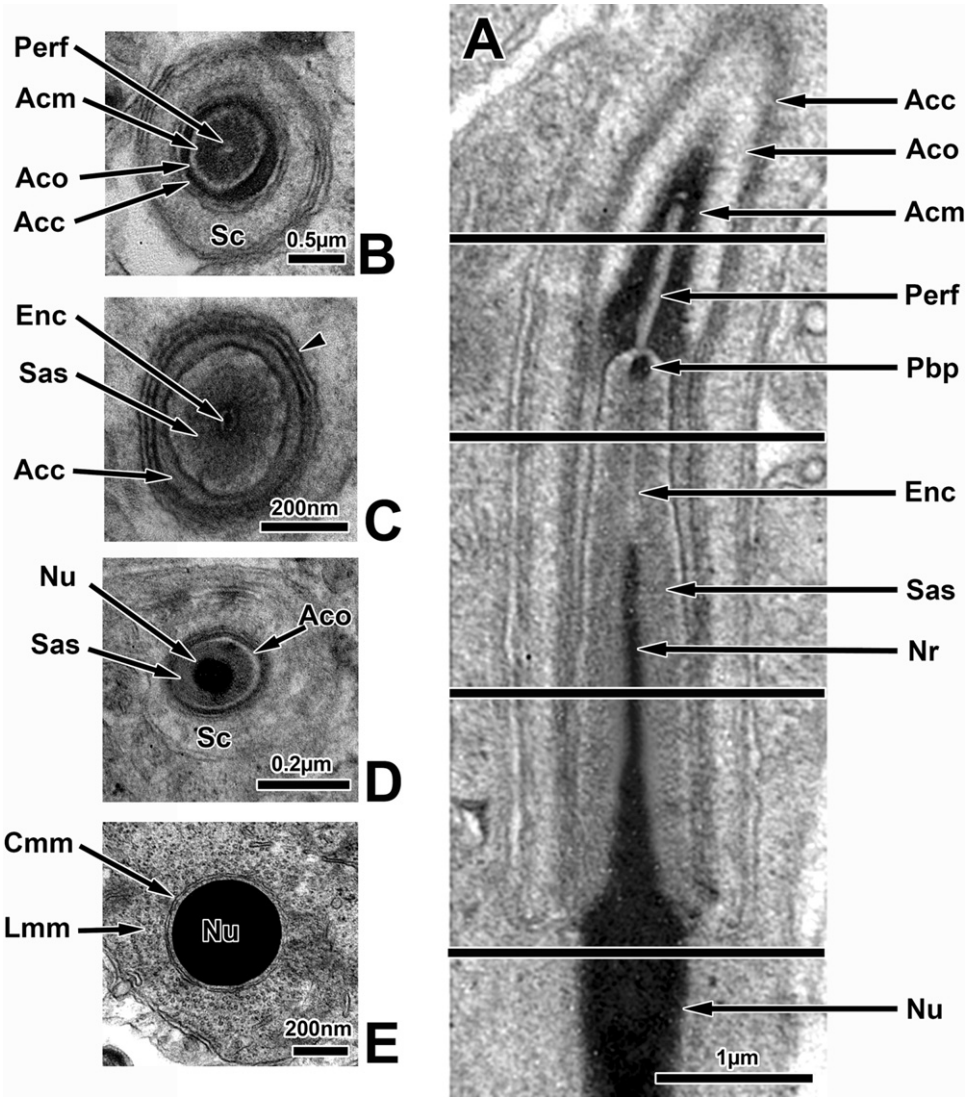

Fig. 8. Transmission electron micrographs of a step 8 spermatid prior to be shed into the lumen during spermiation. Lines indicate approximations of where cross-sectional micrographs (B–E) are taken. (A) Sagittal view of the apical portion of the nucleus and associated acrosome. A dark band of proteins makes up the acrosomal cap (Acc) and surrounds the electron lucent acrosomal cortex (Aco) and inner electron-dense acrosome medulla (Acm). The perforatorium (Perf) lies within the acrosomal medulla and sets on the perforatorial base plate (Pbp). An electron lucent endonuclear canal (Enc) lies apical to the tip of the nucleus (Nu), the nuclear rostrum (Nr), within the subacrosomal space (Sas). (B) Cross-sectional view of the apical acrosome detailing the perforatorium (Perf), acrosomal cortex (Aco) and inner medulla (Acm), the acrosomal cap (Acc), and surrounding Sertoli cell (Sc). (C) Cross-sectional view through the epinuclear lucent zone (Enc) detailing the subacrosomal space (Sas), acrosomal cap (Acc), and Sertoli cell membranes (black arrowhead). (D) Cross-sectional view through the nuclear rostrum detailing the tip of the nucleus (Nu) surrounded by the acrosomal cortex (Aco) subacrosomal space (Sas), and surrounding Sertoli cell (Sc). (E) Cross-sectional view through the nucleus proper (Nu) detailing the surrounding longitudinal (Lmm) and circum-cylindrical (Cmm) microtubules of the manchette. Scale = 200 nm.

them to associate with multiple germ cell stages at once. Up to three Sertoli cells can be found in close association with a single developing *H. turcicus* germ cell, which has previously been described in snakes (Gribbins and Rheubert, in press). The Sertoli cells of *H. turcicus* within the seminiferous epithelium often have different cytoplasmic consistencies and organelle composition, differing even among Sertoli cell clusters, which suggests different functions of individual Sertoli cells. These differing functions could potentially be a result of having multiple germ cell stages within a single region of the seminiferous tubule; however their true biological role is unknown at this time. Although Sertoli cells surround multiple generations of germ cells during development, it seems at least in *H. turcicus* and some snakes (Gribbins and Rheubert, in press) that only one Sertoli cell is in close association with late elongating spermatids.

This study is the first to describe spermiogenesis in a gecko and only one of a handful of studies regarding sperm or sperm development in Gekkonidae. From the above analysis many of the processes of sperm development are highly conserved as suggested by Gribbins and Rheubert, in press. However, when compared with characters of the mature spermatozoa and the process of spermiogenesis it is evident that some differences exist (e.g., presence/absence of epinuclear zone, number of endonuclear canals, where the fibrous sheath begins). It appears as if many morphological features are conserved, and species or lineages are composed of unique combinations of the different features rather than being defined by novel synapomorphies. Although vital attempts at phylogenetic reconstructions and evolutionary hypotheses have been performed (Jamieson et al., 1996; Jamieson, 1999; Rheubert et al., 2010a), with so few taxa being studied to date any elucidation of the evolutionary aspects of spermatozoa and spermiogenesis are premature. Future studies involving spermiogenesis within a wide array of taxa may help to clarify any phylogenetic significance and/or evolutionary trends within Lepidosaurians.

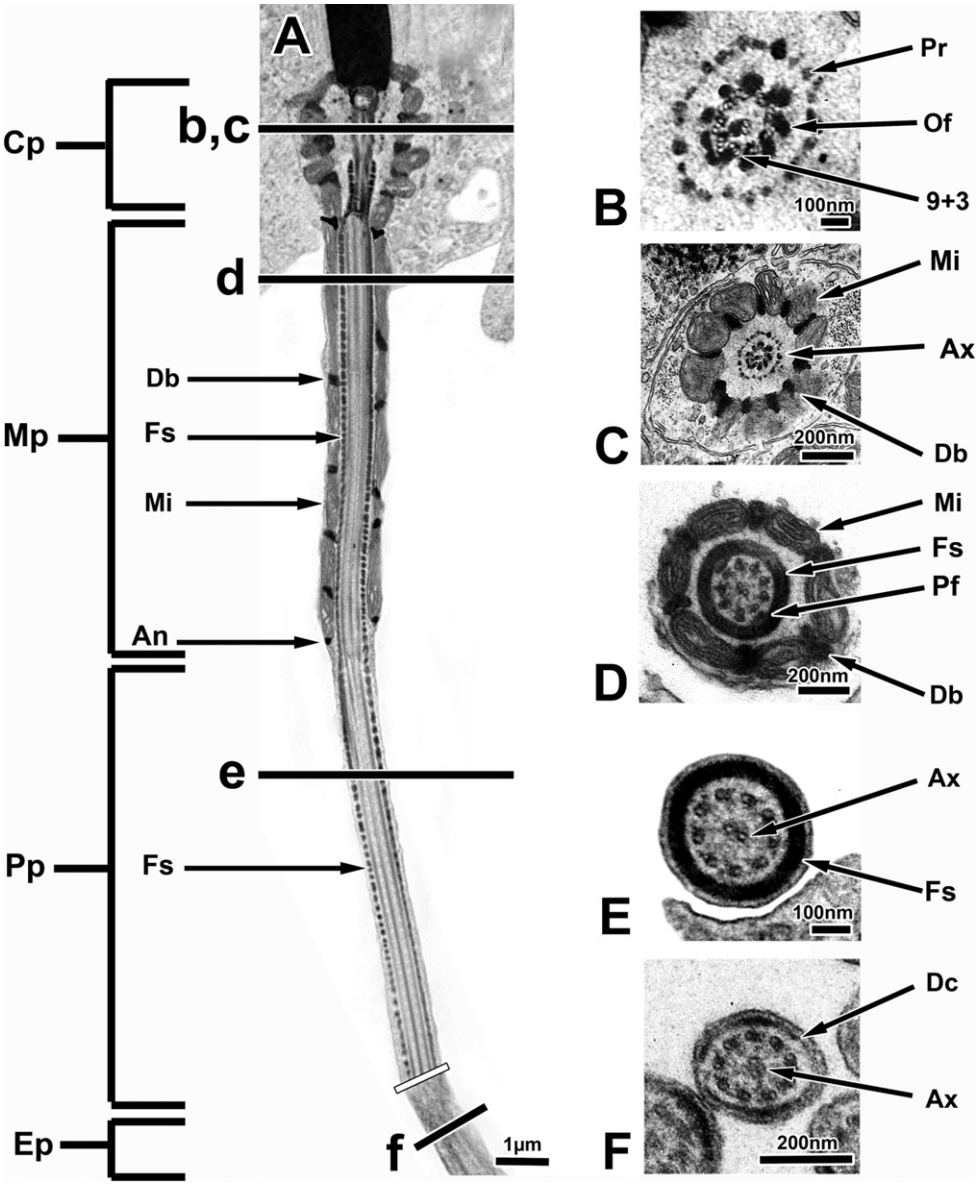

Fig. 9. Transmission electron micrographs of the posterior portion of a step 8 spermatid prior to being shed to the lumen during spermiation. (A) Sagittal view of the posterior step 8 spermatid showing the division into the connecting piece (Cp), midpiece (Mp), principal piece (Pp), and endpiece (Ep). Black lines indicate approximate locations where cross-sectional views were taken. White line indicates where two images were pieced together to provide the full length flagellum. The midpiece fibrous sheath (Fs) begins at the third mitochondrial tier and continues through the principal piece. The midpiece is surrounded by mitochondria (Mi) and dense bodies (Db) and terminates at the annulus (An). (B) Enlarged view of the distal centriole at the connecting piece detailing the protein ring (Pr) surrounding the centriole, the outer fibers (Of) associated with the microtubules, and the 9 + 3 arrangement of the microtubules. (C) Cross-sectional view of the connecting piece detailing axoneme (Ax) and the surrounding mitochondria (Mi) and dense bodies (Db). (D) Cross-sectional view through the midpiece showing the surrounding mitochondria (Mi) and dense bodies (Db). The fibrous sheath (Fs) surrounds the axoneme and peripheral fibers (Pf) are enlarged microtubule doublets 3 and 8. (E) Cross-sectional view through the principal piece showing the 9 + 2 microtubule arrangement of the axoneme (Ax) and the surrounding fibrous sheath (Fs). (F) Cross-sectional view through the endpiece showing the absence of the fibrous sheath surround the distal centriole (Dc) and the 9 + 2 microtubule arrangement of the axoneme (Ax).

Acknowledgements

The authors would like to thank Chris Murray for his helpful comments on an earlier draft of this manuscript. Funding was provided by National Science Foundation Grant #DEB-0809831 to DMS and in part by Wittenberg University.

References

Al-Dokhi, O.A., 2004. Electron microscopic study of sperm tail differentiation in the lizard *Bunopus tuberculatus* (Squamata, Reptilia). Saud. J. Biol. Sci. 11, 111–117.

Al-Dokhi, O.A., 2009. Morphogenesis of the acrosomal vesicle during spermiogenesis in the House Gecko, *Ptyodactylus hasselquistii* (Squamata, Reptilia). Int. J. Zool Res. 5, 136–149.

Butler, R.D., Gabri, M.S., 1984. Structure and development of the sperm head in the lizard *Podarcis* (=Lacerta) *taurica*. J. Ultrastruct. Res. 88, 261–274.

Carcupino, M., Corso, G., Pala, M., 1989. Spermiogenesis in *Chalcides ocellatus tiligugu* (Gmelin) (Squamata, Scincidae): an electron microscope study. Italian J. Zool. 56, 119–124.

Clark, A.W., 1967. Some aspects of spermiogenesis in a lizard. Am. J. Anat. 121, 369–400.

Colli, G.R., Teixeira, R.D., Scheltinga, D.M., Mesquita, D.O., Wiederhecker, H.C., Báo, S.N., 2007. Comparative study of sperm ultrastructure of five species of teiid lizards (Teiidae, Squamata), and *Cercosaura ocellata* (Gymnophthalmidae, Squamata). Tissue Cell 39, 59–78.

Cunha, L.D., Tavares-Bastos, L., Báo, S.N., 2008. Ultrastructural description and cytochemical study of the.spermatozoon of *Crotalus durissus* (Squamata, Serpentes). Micron 39, 915–925.

Del Conte, E., 1976. The subacrosomal granule and its evolution during spermiogenesis in a lizard. Cell Tissue Res. 171, 483–498.

Eckstut, M.E., Lemons, E.R., Sever, D.M., 2009. Annual dynamics of sperm production and storage in the Mediterranean Gecko, *Hemidactylus turcicus*, in the southeastern United States. Amphibia-Reptilia 30, 45–56.

Fawcett, D.W., 1970. A comparative view of sperm ultrastructure. Biol. Reprod. 2, 90–127.

Ferreira, A., Dolder, H., 2002. Ultrastructural analysis of spermiogenesis in *Iguana iguana* (Reptilia: Sauria: Iguanidae). Eur. J. Morphol. 40, 89–99.

Ferreira, A., Dolder, H., 2003. Sperm ultrastructure and spermatogenesis in the lizard, *Tropidurus itambere*. Biocell 27, 353–362.

Furieri, P., 1970. Sperm morphology in some reptiles: Squamata and Chelonia. In: accetti, B. (Ed.), Comparative Spermatology. Academic Press Inc., New York, pp. 115–132.

Gribbins, K.M., Gist, D.H., 2003. Cytological evaluation of spermatogenesis in the Red-eared Slider, *Trachemys scripta*. J. Morphol. 255, 337–346.

Gribbins, K.M., Rheubert, J.L. The ophidian testis, spermatogenesis, and mature spermatozoa. In: Aldridge, R.D., Sever, D.M. (Eds.), Reproductive Biology and Phylogeny of Snakes. Science Publishers Inc., Enfield, NH, in press.

Gribbins, K.M., Mills, E.M., Sever, D.M., 2007. Ultrastructural examination of spermiogenesis within the testis of the Ground Skink, *Scincella laterale* (Squamata, Sauria, Scincidae). J. Morphol. 268, 181–192.

Gribbins, K.M., Rheubert, J.L., Anzalone, M.L., Siegel, D.S., Sever, D.M., 2010. Ultrastructure of spermiogenesis in the Cottonmouth *Agkistrodon piscivorus* (Squamata: Viperidae: Crotalinae). J. Morphol. 271, 293–304.

Han, D., Zhou, K., Bauer AM, 2004. Phylogenetic relationships among gekkotan lizards inferred from C-mos nuclear DNA sequences and a new classification of the Gekkot. Biol. J. Linn. Soc. 83, 353–368.

Healy, J.M., Jamieson, B.G.M., 1992. The phylogenetic position of the Tuatara, Sphenodon (Sphenodontida, Amniota), as indicated by cladistic analysis of the ultrastructure of spermatozoa. Philos. Trans. Biol. Sci. 335, 207–219.

Healy, J.M., Jamieson, B.G.M., 1994. The ultrastructure of spermatogenesis and epididymal spermatozoa of the Tuatara, *Sphenodon punctatus* (Sphenodontida, Amniota). Philos. Trans. Biol. Sci. 344, 187–199.

Hondo, E., Kurohmaru, M., Toriba, M., Hayashi, Y., 1994. Seasonal changes in spermatogenesis and ultrastructure of developing spermatids in the Japanese rat snake, *Elaphe climacophora*. J. Vet. Med. Sci. 56, 836–840.

Jamieson, B.G.M., 1981. Ultrastructure of spermatogenesisis in *Phreodrilus* (Phreodrilidae, Oligochaeta, Annelidae). Journal of Zoology 194, 393–408.

Jamieson, B.G.M., 1991. Fish Evolution and Systematics: Evidence from Spermatozoa. Cambridge University Press, Cambridge, UK.

Jamieson, B.G.M., 1995. The ultrastructure of spermatozoa of the Squamata (Reptilia) with phylogenetic considerations. In: Jamieson, B.G.M., Ausio, J., Justine, J.-L. (Eds.), Advances in Spermatozoal Phylogeny and Taxonomy, vol. 166. Mémoires du Muséum national d'Histoire Naturelle, Paris, pp. 359–383.

Jamieson, B.G.M., 1999. Spermatozoal phylogeny of the Vertebrata. In: Gagnon, C. (Ed.), The Male Gamete: From Basic Science to Clinical Applications. Cache River Press, Vienna, USA, pp. 303–331.

Jamieson, B.G.M., Oliver, S.C., Scheltinga, D.M., 1996. The ultrastructure of the spermatozoa of squamata. I. Scincidae, Gekkonidae, and Pygopodidae (Reptilia). Acta Zool. (Stockholm) 77, 85–100.

Moreno, R.D., Ramalho-Santos, J., Sutovsky, P., Chan, E.K.L., Schatten, G., 2000. Vesicular traffic and Golgi apparatus dynamics during mammalian spermatogenesis: implications for acrosome architecture. Biol. Reprod. 63, 89–98.

Mubarak, M., 2006. Ultrastructure of sperm tail differentiation of the lizard *Stenodactylus dorie* (Squamata, Reptilia). J. Biol. Sci. 6, 187–192.

Mruk, D.D., Silvestrini, B., Yan Cheng, C., 2008. Anchoring junctions as drug targets: role in contraceptive development. Pharmacol. Rev. 60, 146–180.

Newton, W.D., Trauth, S.E., 1992. Ultrastructure of the spermatozoon of the lizard *Cnemidophorus sexlineatus* (Sauria: Teiidae). Herpetologica 48, 330–343.

Rheubert, J.L., Poldemann, E.H., Eckstut, M.E., Collier, M.H., Sever, D.M., Gribbins, K.M., 2009. Temporal germ cell development strategy during mixed spermatogenesis within the male Mediterranean Gecko, *Hemidactylus turcicus* (Reptilia: Gekkonidae). Copeia 4, 793–800.

Rheubert, J.L., McMahan, C.D., Sever, D.M., Bundy, M.R., Siegel, D.S., Gribbins, K.M., 2010a. Ultrastructure of the reproductive system of the Black Swamp Snake (*Seminatrix pygaea*). VII. Spermatozoon morphology and evolutionary trends of sperm characters in snakes. J. Syst. Zool. Evol. Res. 48, 366–375.

Rheubert, J.L., Sever, D.M., Geheber, A.D., Siegel, D.S., 2010b. Proximal testicular ducts of the Mediterranean Gecko (*Hemidactylus turcicus*). Anat. Rec. 293, 2176–2792.

Rheubert, J.L., Wilson, B.S., Wolf, K.W., Gribbins, K.M., 2010c. Ultrastructural study of spermiogenesis in the Jamaican Gray Anole, *Anolis lineatopus* (Reptilia: Polychrotidae). Acta Zool. (Stockholm) 91, 484–494.

Röll, B., von Düring, M.U.G., 2008. Sexual characteristics and spermatogenesis in males of the parthenogenetic gecko *Lepidoctylus lugubris* (Reptilia, Gekkonidae). Zoology 5, 385–400.

Russell, L.D., Ettlin, R.A., Hikim, A.M.P., Clegg, E.D., 1990. Histological and Histopathological Evaluation of the Testis. Cache River Press, Clearwater, FL.

Talbot, P., 1991. Compartmentalization in the acrosome. In: Baccetti, B. (Ed.), Comparative Spermatology – 20 Years After. Raven Press, New York, pp. 225–259.

Tavares-Bastos, L., Teixeira, R.D., Colli, G.R., Báo, S.N., 2002. Polymorphism in the sperm ultrastructure among four species of lizards in the genus *Tupinambis* (Squamata: Teiidae). Acta Zool. (Stockholm) 83, 297–307.

Tavares-Bastos, L., Cunha, L.D., Colli, G.R., Báo, S.N., 2007. Ultrastructure of spermatozoa of scolecophidian snakes (Lepidosauria, Squamata). Acta Zool. (Stockholm) 88, 189–197.

Teixeira, R.D., Colli, G.R., Báo SN, 1999a. The ultrastructure of the spermatozoa of the lizard *Micrablepharus maximiliani* (Squamata, Gymnophthalmidae), with considerations on the use of sperm ultrastructure characters in phylogenetic reconstruction. Acta Zool. (Stockholm) 80, 47–59.

Teixeira, R.D., Colli, G.R., Báo, S.N., 1999b. The ultrastructure of spermatozoa of the lizard *Polychrus acutirostris* (Squamata, Polychrotidae). J. Submicrosc. Cytol. Pathol. 31, 387–395.

Teixeira, R.D., Scheltinga, D.M., Trauth, S.E., Colli, G.R., Báo, S.N., 2002. A comparative ultrastructural study of spermatozoa of the teiid lizards *Cnemidophorus gularis gularis*, *Cnemidophorus ocellifer*, and *Kentropyx altamazonica* (Reptilia, Squamata, Teiidae). Tissue Cell 34, 135–142.

Tourmente, M., Giojalas, L., Chiaraviglio, M., 2008. Sperm ultrastructure of *Bothrops alternatus* and *Bothrops diporus* (Viperidae, Serpentes), and its possible relation to the reproductive features of the species. Zoomorphology 127, 241–248.

Ventela, S., Toppari, J., Parvinen, M., 2003. Intercellular organelle traffic through cytoplasmic bridges in early spermatids of the rat: Mechanism of haploid gene product sharing. Mol. Biol. Cell 14, 2768–2780.

Vieira, G.H.C., Wiederhecker, H.C., Colli, G.R., Báo, S.N., 2001. Spermiogenesis and testicular cycle of the lizard *Tropidurus torquatus* (Squamata, Tropiduridae) in the Cerrado of central Brazil. Amphibia-Reptilia 22, 217–233.

Vieira, G.H.C., Colli, G.R., Báo, S.N., 2004. The ultrastructure of the spermatozoon of the lizard *Iguana iguana* (Reptilia, Squamata, Iguanidae) and the variability of sperm morphology among iguanian lizards. J. Anat. 204, 451–464.

Vieira, G.H.C., Colli, G.R., Báo, S.N., 2005. Phylogenetic relationships of corytophanid lizards (Iguania, Squamata, Reptilia) based on partitioned and total evidence analyses of sperm morphology, gross morphology, and DNA data. Zool. Scripta 34, 605–625.

Vieira, G.H.C., Cunha, L.D., Scheltinga, D.M., Glaw, F., Colli, G.R., Báo, S.N., 2007. Sperm ultrastructure of hoplocercid and oplurid lizards (Sauropsida, Squamata, Iguania) and the phylogeny of Iguania. J. Zool. Syst. Evol. Res. 10, 439–469.